ELSEVIER

Since January 2020 Elsevier has created a COVID-19 resource centre with free information in English and Mandarin on the novel coronavirus COVID-19. The COVID-19 resource centre is hosted on Elsevier Connect, the company's public news and information website.

The celecoxib derivative kinase inhibitor AR-12 (OSU-03012) inhibits Zika virus via down-regulation of the PI3K/Akt pathway and protects Zika virus-infected A129 mice: A host-targeting treatment strategy

Jasper Fuk-Woo Chan[a,b,c,d,e,i,*,1,2], Zheng Zhu[b,1], Hin Chu[b,1], Shuofeng Yuan[b], Kenn Ka-Heng Chik[b], Chris Chung-Sing Chan[b], Vincent Kwok-Man Poon[b], Cyril Chik-Yan Yip[b], Xi Zhang[b], Jessica Oi-Ling Tsang[b], Zijiao Zou[b], Kah-Meng Tee[b], Huiping Shuai[b], Gang Lu[d,e,f,g], Kwok-Yung Yuen[a,b,c,d,e,h,i,**,2]

[a] State Key Laboratory of Emerging Infectious Diseases, The University of Hong Kong, Pokfulam, Hong Kong Special Administrative Region
[b] Department of Microbiology, Li Ka Shing Faculty of Medicine, The University of Hong Kong, Pokfulam, Hong Kong Special Administrative Region
[c] Carol Yu Centre for Infection, The University of Hong Kong, Pokfulam, Hong Kong Special Administrative Region
[d] Hainan Medical University, The University of Hong Kong Joint Laboratory of Tropical Infectious Diseases, Hainan Medical University, Haikou, Hainan, China
[e] The University of Hong Kong, Pokfulam, Hong Kong Special Administrative Region
[f] Department of Pathogen Biology, Hainan Medical University, Haikou, Hainan, 571101, China
[g] Key Laboratory of Translational Tropical Medicine, Hainan Medical University, Haikou, Hainan, 571101, China
[h] The Collaborative Innovation Center for Diagnosis and Treatment of Infectious Diseases, The University of Hong Kong, Pokfulam, Hong Kong Special Administrative Region
[i] The University of Hong Kong-Shenzhen Hospital, Shenzhen, China

ARTICLE INFO

ABSTRACT

Zika virus (ZIKV) is a human-pathogenic flavivirus that has recently emerged as a global public health threat. ZIKV infection may be associated with congenital malformations in infected fetuses and severe neurological and systemic complications in infected adults. There are currently limited treatment options for ZIKV infection. AR-12 (OSU-03012) is a celecoxib derivative cellular kinase inhibitor that has broad-spectrum antiviral activities. In this study, we investigated the antiviral activity and mechanism of AR-12 against ZIKV. We evaluated the *in vitro* anti-ZIKV activity of AR-12, using cell protection and virus yield reduction assays, in multiple clinically relevant cell lines, and the *in vivo* treatment effects of AR-12 in a lethal mouse model using type I interferon receptor-deficient A129 mice. AR-12 inhibited ZIKV strains belonging to both the African and Asian/American lineages in Huh-7 and/or neuronal cells. AR12's IC_{50} against ZIKV was consistently $< 2\,\mu M$ in these cells. ZIKV-infected A129 mice treated with intraperitoneally or orally administered AR-12 had significantly higher survival rate (50.0%–83.3% vs 0%, $P < 0.05$), less body weight loss, and lower blood and tissue ZIKV RNA loads than untreated control A129 mice. These anti-ZIKV effects were likely the results of down-regulation of the PI3K/Akt pathway by AR-12. Clinical trials using the clinically available and broad-spectrum AR-12 as an empirical treatment should be considered especially for patients residing in or returning from areas endemic of ZIKV and other arboviral infections who present with an acute undifferentiated febrile illness.

1. Introduction

Globalization and climate changes continue to reshape the geographical distribution of humans, animals, vectors, and microbes, and allow their mixing to occur at an unprecedentedly high frequency (Chan et al., 2013b). These have led to interspecies transmission of

---

numerous emerging pathogens in the past few decades, such as avian influenza viruses, severe acute respiratory syndrome and Middle East respiratory syndrome coronaviruses, Ebola virus, and other viruses causing hemorrhagic fever (Chan et al., 2015; MacNeil and Rollin, 2012; Marsh and Wang, 2012; To et al., 2013; To et al., 2015). The latest emerging viral epidemic that was declared as an international health emergency is the one caused by Zika virus (ZIKV) (Musso and Gubler, 2016). ZIKV is a human-pathogenic flavivirus that has been neglected until recently, when it was found that ZIKV infection may be associated with severe clinical complications, including congenital microcephaly and other anomalies, neurological complications such as Guillain-Barre syndrome and meningoencephalitis, ophthalmological defects, auditory impairment, and rarely, multi-organ involvement and death (Chan et al., 2016b; Musso and Gubler, 2016).

ZIKV infection, similar to other emerging viral infections, may have non-specific clinical manifestations during the early phase of the disease (Chan et al., 2016b; Duffy et al., 2009). For example, ZIKV infection may manifest as an acute febrile illness with rash and systemic upset which may be indistinguishable from dengue fever and other viral hemorrhagic fever syndromes (Chan et al., 2016b; Duffy et al., 2009). Moreover, ZIKV may co-circulate with other viruses in the same geographical regions and co-infect the same patient (Musso and Gubler, 2016). As in the case of most other emerging viral infections, there are currently limited treatment options proven to be effective and safe for ZIKV infection. Thus, broad-spectrum agents that can be used as empirical treatment for patients with an acute undifferentiated febrile illness before the diagnosis is confirmed by laboratory tests are urgently needed.

An important group of drugs that have broad-spectrum antiviral activities are agents that target host pathways or enzymes that are involved in the replication cycles of different viruses (Zumla et al., 2016). For example, host cellular kinases have been increasingly implicated in the pathogenesis of viral infections as they may be exploited by viruses to facilitate their own replication (Chu and Yang, 2007; Linero and Scolaro, 2009; Saeed et al., 2008; Urata et al., 2012). For flaviviruses, the phosphatidylinositol 3 kinase/protein kinase B (PI3K/Akt) pathway has been shown to enhance viral replication through counteracting virus-induced cellular apoptosis (Lee et al., 2005; Tsai et al., 2014). AR-12 (OSU-03012), an FDA-approved investigational new drug (IND) compound, is a celecoxib derivative kinase inhibitor that does not inhibit cyclooxygenase activity, but instead downregulates the PI3K/Akt pathway which are involved in multiple cell signaling pathways (Chen et al., 2017; Mohr et al., 2015). AR-12 has been evaluated in phase I clinical trials as an anticancer agent in adult patients with advanced or recurrent solid tumors or lymphoma (Clinical Trials registration no. NCT00978523).

In addition to its anti-cancer effects, AR-12 has exhibited *in vitro* and/or *in vivo* antimicrobial activities against a wide range of pathogens. These microbes included intracellular bacteria (*Salmonella enterica* and *Francisella tularensis*), fungi (*Candida albicans,* non-albicans *Candida* sp., *Cryptococcus neoformans*, *Fusarium* sp., mucorales, *Blastomyces dermatitidis*, *Histoplasma capsulatum*, and *Coccidioides immitis*), parasite (*Leishmania donovani*), and viruses (Lassa, Marburg, and Ebola viruses) (Chiu et al., 2009a; Chiu et al., 2009b; Collier et al., 2016; Koselny et al., 2016; Mohr et al., 2015). Importantly, the European Commission has designated AR-12 as an orphan drug that could be used clinically in combination with other anti-infective agents for treatment of cryptococcosis (with fluconazole) and tularemia (with gentamicin) (Booth et al., 2016). These clinical experiences make AR-12 a clinically readily available drug for emerging infectious diseases lacking effective treatment options. Recently, AR-12 was reported to have *in vitro* and *in vivo* antiviral activity against dengue virus (DENV), another flavivirus that is closely related to the emerging ZIKV (Chen et al., 2017; Hassandarvish et al., 2017). We therefore hypothesized that this broad-spectrum host-targeting antiviral drug may also exhibit inhibitory activity against ZIKV. In this study, we evaluated the *in vitro*

and *in vivo* antiviral activity of AR-12 against ZIKV and investigated the mechanism of AR-12's anti-ZIKV activity.

2. Materials and methods

2.1. Ethics and biosafety

The animal experiments were approved by the Committee on the Use of Live Animals in Teaching and Research of The University of Hong Kong and performed according to established safety protocols in the biosafety level-2 laboratory at Department of Microbiology, The University of Hong Kong.

### 2.2. Virus strains, cell lines, and drug compounds

ZIKV-PR (Puerto Rico strain PRVABC59) was isolated from a patient in the recent South American epidemic (kindly provided by Brandy Russell and Barbara Johnson, Centers for Disease Control and Prevention, USA). ZIKV-GD was isolated from a Chinese patient who returned to Guangdong after being infected by ZIKV while traveling to the Americas (kindly provided by George F. Gao, Chinese Academy of Sciences, China). ZIKV-U (976 Uganda strain) was isolated from a nonhuman primate in Uganda in 1947 (kindly provided by Tatjana Avšič Županc, University of Ljubljana, Slovenia, the European Virus Archive). The virus strains were cultured and titrated as we previously described (Chan et al., 2016c; Yuan et al., 2017). The U251 and SF268 cell lines were obtained from American Type Culture Collection, and the Huh-7 cell line was obtained from JCRB cell bank of Okayama University, Japan (Chan et al., 2016c). AR-12 and the Akt inhibitor (Akt Inhibitor VIII) were purchased from InvivoGen (SanDiego, CA, USA) and Millipore (Burlington, MA, USA), respectively. ON-TARGETplus human Akt siRNA and ON-TARGETplus non-targeting siRNA were purchased from Dharmacon (Lafayette, CO, USA).

2.3. CellTiter-Glo® luminescent cell viability assay

The 50% effective cytotoxic concentration (CC_{50}) of AR-12 in Huh-7, U251, and SF268 cells and the cell protection effects of AR-12 against ZIKV infection in these cell lines were determined by the CellTiter-Glo® luminescent cell viability assay (PromegaCorporation, Madison, WI, USA) according to the manufacturer's instructions and as previously described (Mohr et al., 2015). For determination of CC_{50} of AR-12 treatment without ZIKV infection, the cells were treated with different concentrations of AR-12 (0–20 μM) for 48 h. For cell protection effects, the cells were infected by ZIKV-PR at 0.50 multiplicity of infection (MOI) for 1 h and then treated with dimethyl sulfoxide (DMSO) (ie: 0 μM AR-12) or up to 3 μM AR-12 for 48 h. After 48 h, the reconstituted CellTiter-Glo® reagent was added to the cells according to the manufacturer's instructions. The luminescent signal was detected by the Victor X3 2030 Multilabel Reader (PerkinElmer) according to the manufacturer's instructions.

2.4. Antiviral evaluation of AR-12 in cell culture

The antiviral activity of AR-12 against ZIKV was evaluated in cell culture as previously described (Chan et al., 2017a; Yuan et al., 2017). Briefly, ZIKV-infected Huh-7, U251, and SF268 cells (MOI = 0.05) were treated with different concentrations of AR-12 or DMSO. The cell culture supernatants were then collected at 24 h post-inoculation (hpi), followed by total nucleic acid extraction and quantitative reverse transcription-PCR (qRT-PCR) as previously described (Chan et al., 2016c; Chan et al., 2017b). Additionally, U251 cells were inoculated with high MOI of ZIKV (MOI = 1) for 1 h. After the virus inoculum was removed, the cells were washed and cultured in fresh medium containing different concentrations of AR-12 or DMSO. At 24 hpi, the supernatants were collected and subsequently applied for virus titration
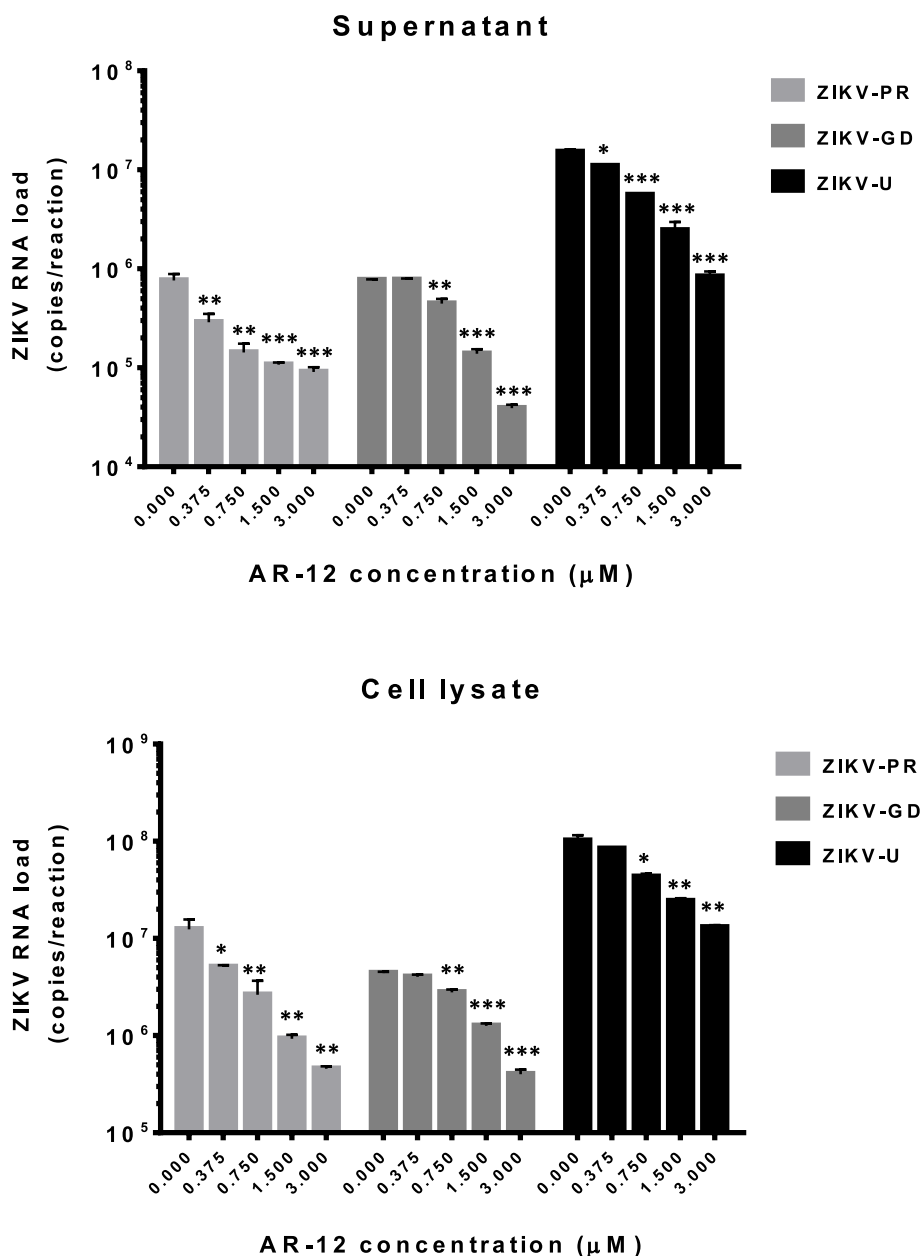
Fig. 1. AR-12 inhibits the replication of ZIKV strains belonging to both the Asian/American and African lineages in Huh-7 cells. Dose-dependent reduction of ZIKV RNA load was observed at 24 h after ZIKV-PR, ZIKV-GD, or ZIKV-U inoculation (0.05 MOI) in Huh-7 cells with 0–3 μM AR-12. All experiments were performed in triplicates in three independent experiments for confirmation. * denotes $P < 0.05$, ** denotes $P < 0.01$, and *** denotes $P < 0.001$ (compared with the DMSO control group by Student's t-test). Data are presented as mean values ± standard deviations (error bars). Abbreviations: ZIKV, Zika virus.

using both qRT-PCR and plaque assay. The half maximal inhibitory concentration (IC$_{50}$) was calculated using Sigma plot in an Excel add-in ED50V10 as we previously described (Chan et al., 2013a; Chan et al., 2017a; Chan et al., 2017b).

2.5. Flow cytometry

To more thoroughly compare the differences between the percentage of cells infected by ZIKV in AR-12-treated versus untreated samples, flow cytometry and immunostaining was performed as we previously described with slight modifications (Chu et al., 2014; Chu et al., 2016). Briefly, U251 cells were infected with ZIKV-PR at 0.50 MOI or were mock-infected for 1 h at 37 °C. After 1 h, the inoculum was removed and the cells were washed with phosphate-buffered saline (PBS). Dulbecco's Modified Eagle Medium (DMEM) with 3 μM AR-12 or 1%

DMSO (Sigma-Aldrich, St.Louis, MO, USA) was then added to the cells. At 24 hpi, the cells were detached by using 10 mM ethylenediaminetetraacetic acid (EDTA)/PBS and fixed in 4% paraformaldehyde. For immunostaining, the cells were first permeabilized with 0.1% Triton X-100 in PBS and then blocked with 2% fetal bovine serum (FBS) in PBS. ZIKV was detected with a mouse anti-ZIKV-NS1 primary antibody (Abcam, Cambridge, United Kingdom) or the mouse anti-pan-flavivirus primary antibody 4G2 (Millipore) and Alexa Fluor 488 goat anti-mouse immunoglobulin (IgG) (Invitrogen, Carlsbad, CA, USA) as the secondary antibody. Flow cytometry was performed using a BD FACSCanto II flow cytometer (BD Biosciences, San Jose, CA, USA) and the data were analyzed using FlowJo vX (Tree Star).
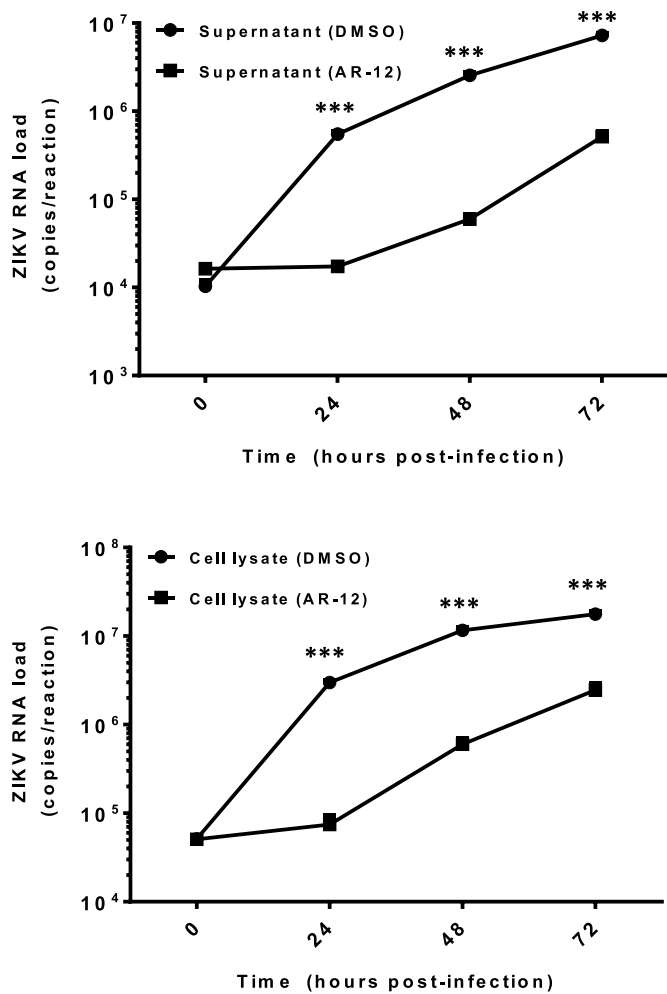
Fig. 2. AR-12 effectively inhibits multi-cycle replication of ZIKV *in vitro*. Differential viral kinetics of ZIKV in Huh-7 cells with or without AR-12 from 0 to 72 hpi. The ZIKV-PR RNA load in both the culture supernatant (top) and cell lysate (bottom) of the AR-12-treated (3 μM) samples were consistently ~1.0–1.5 logs lower than those of the DMSO-treated controls at different time points (24, 48, and 72 hpi). All experiments were performed in triplicates in three independent experiments for confirmation. *** denotes $P < 0.001$ (compared with the DMSO control group at the corresponding time point by Student's *t*-test). Data are presented as mean values ± standard deviations (error bars). Abbreviations: DMSO, dimethyl sulfoxide; hpi, hours post-inoculation; ZIKV, Zika virus.

2.6. Western blot

Huh-7 cells were lysed with radioimmunoprecipitation assay (RIPA) lysis buffer (Thermo Fisher Scientific, Waltham, MA, USA) with protease inhibitors cocktail (Sigma-Aldrich). Western blotting was performed as we previously described with slight modifications (Chan et al., 2016a). Briefly, proteins were separated with electrophoresis on 10% sodium dodecyl sulfate (SDS) gels and transferred onto polyvinylidene difluoride (PVDF) membranes. The PVDF membranes were subsequently blocked with 3% bovine serum albumin (BSA) for 1 h at room temperature and incubated with the primary antibodies at 4 °C overnight. On the next day, the membranes were washed thrice with 0.1% PBS with Tween 20 buffer and incubated with peroxidase-conjugated secondary antibodies for 2 h at room temperature. The protein bands on the membranes were visualized by using horseradish peroxidase (HRP) substrate (Bio-Rad, Hercules, CA, USA). The antibodies used for Western blotting in this study were as follows: anti-Akt 1 antibody [M1843] (ab108202, Abcam), anti-pan-Akt (phosphor T308)
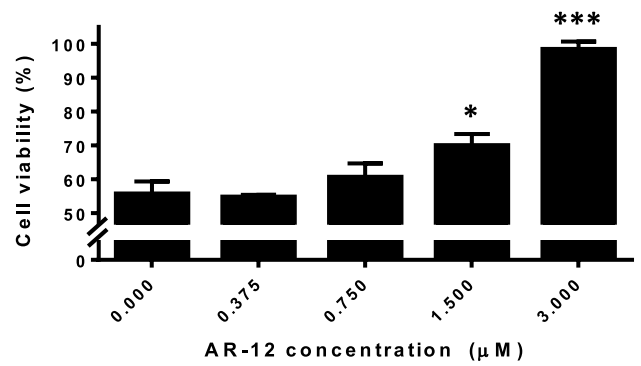
Fig. 3. AR-12 provided cell protection effects against ZIKV infection. Cell viability assay showing dose-dependent increase in the percentage of viable cells in AR-12-treated Huh-7 cells. All experiments were performed in triplicates in three independent experiments for confirmation. * denotes $P < 0.05$ and *** denotes $P < 0.001$ (compared with the DMSO control group by Student's *t*-test). Data are presented as mean values ± standard deviations (error bars).
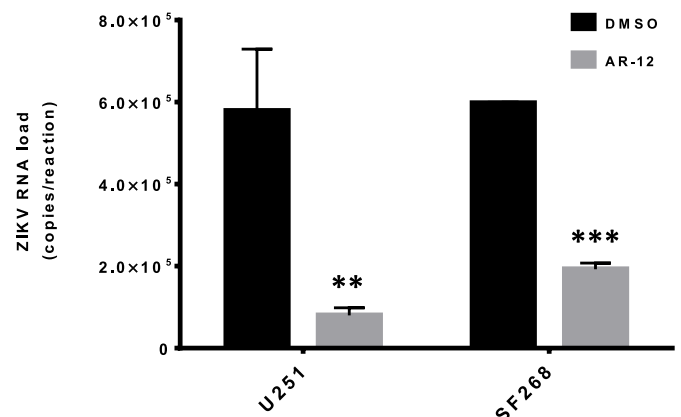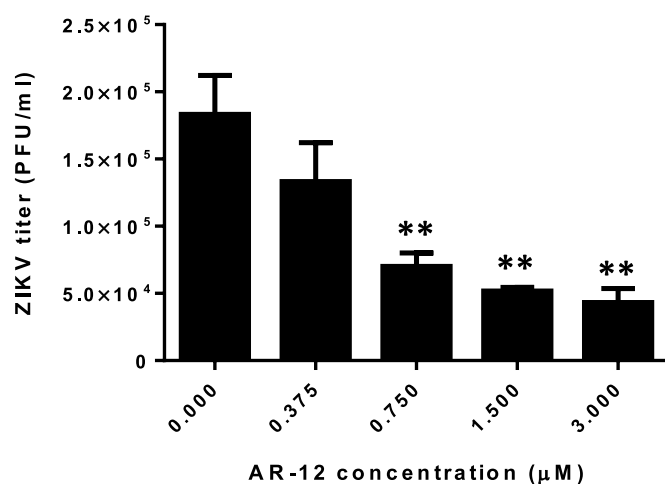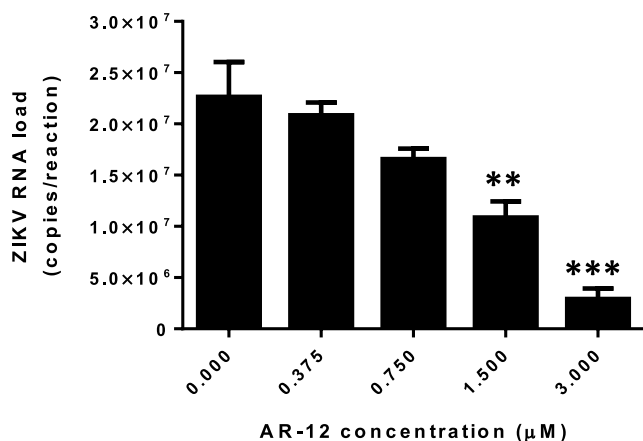

Fig. 4. AR-12 inhibits ZIKV replication in neuronal cells. Significant reduction of ZIKV-PR (MOI = 0.05) RNA load was observed at 24 hpi in U251 and SF268 cells with 3 μM AR-12 compared with DMSO (0 μM AR-12) control. All experiments were performed in triplicates in three independent experiments for confirmation. ** denotes $P < 0.01$ and *** denotes $P < 0.001$ (compared with the DMSO control group by Student's *t*-test). Data are presented as mean values ± standard deviations (error bars). Abbreviations: DMSO, dimethyl sulfoxide; hpi, hours post-inoculation; ZIKV, Zika virus.

antibody (ab38449, Abcam), goat anti-rabbit IgG (H + L) secondary antibody (HRP 65–6120, Thermo Fisher), and goat anti-mouse IgG (H + L) secondary antibody (HRP 62–6520, Thermo Fisher).

2.7. Akt inhibitor and small interfering RNA (siRNA) knockdown

In the Akt inhibitor assay, Huh-7 cells were inoculated with ZIKV for 1 h at 37 °C. At 1 hpi, the inoculum was removed and the cells were washed with PBS. DMEM containing 15 μM Akt inhibitor or 1% DMSO was added to the ZIKV-infected cells. At 24 hpi, the supernatants were harvested in RLT buffer and RNA was extracted with the EZ1 RNA tissue mini kit (Qiagen, Hilden, Germany). The viral load was then quantified with qRT-PCR as we previously described (Chan et al., 2016c; Chan et al., 2017b). In the siRNA knockdown assay, transfection of siRNA on Huh-7 cells was performed using Lipofectamine® RNAiMAX (Thermo Fisher Scientific) as we previously described with slight modifications (Chan et al., 2016a). Briefly, 70 nM Akt siRNA or scramble siRNA was mixed with RNAiMAX and Opti-MEM, which was then used to transfect Huh-7 cells. At 24 h post-transfection, the siRNA-

Fig. 5. AR-12 inhibits ZIKV replication at high MOI. Dose-dependent reduction of ZIKV-PR (MOI = 1) RNA load in qRT-PCR (top) and virus titer in plaque assay (bottom) in U251 cells with different concentrations of AR-12 compared with DMSO (0 μM AR-12) control. All experiments were performed in triplicates in three independent experiments for confirmation. * denotes $P < 0.05$ and ** denotes $P < 0.01$ (compared to the DMSO control group by Student's *t*-test). Data are presented as mean values ± standard deviations (error bars). Abbreviations: ZIKV, Zika virus.

transfected cells were inoculated with ZIKV for 1 h at 37 °C. At 1 hpi, the inoculum was removed and the cells were washed with PBS. DMEM was then added to the cells. At 24 hpi, the supernatants were harvested in RLT buffer and RNA was extracted with the EZ1 RNA tissue mini kit (Qiagen). The viral RNA load was then quantified with qRT-PCR as we previously described (Chan et al., 2016c; Chan et al., 2017b).

2.8. A129 mouse model for ZIKV infection and in vivo evaluation of AR-12 treatment

The type I interferon receptor-deficient lethal A129 mouse model for ZIKV infection was performed as previously described with slight modifications (Dowall et al., 2016; Guo et al., 2018). Briefly, 4-6-week-old A129 mice (Mutant Mouse Resource Research Centers, USA) were randomly divided into different groups to receive AR-12 treatment or sham treatment (n = 12-24/group). Additional groups of uninfected mice receiving intraperitoneal or oral AR-12 treatment were also included as controls (Table S1). The mice were inoculated subcutaneously with 8×10^6 plaque-forming units (PFU) (in 80 μl PBS) of ZIKV-PR under anesthesia at 0 days post-infection (dpi). Each mouse then

received 1 dose of intraperitoneally administered AR-12 (25 mg/kg intraperitoneally or 200 mg/kg orally by oral gavage suspended in PBS with 0.5% methylcellulose-0.1% Tween 80) or sham treatment (PBS) at 1 hpi or 48 hpi as previously described (Table S1) (Chen et al., 2017; Lee et al., 2009). The mice were monitored three times per day for body weight change and clinical signs of disease as previously described (Dowall et al., 2016). Six (12 for sham treatment control group) mice in each group were euthanized when there was ≥20% weight loss or ≥10% weight loss with ≥1 clinical sign or at 6 dpi (the expected day of death of all untreated control mice). Their blood and organ tissues were collected for viral load studies as previously described (Chan et al., 2016d; Yuan et al., 2017). The survival of the other mice was monitored until 14 dpi.

2.9. Statistical analysis

All data were analyzed with GraphPad Prism software (GraphPad Software, Inc) as we previously described (Chan et al., 2016d). Kaplan-Meier survival curves were analyzed by the log rank test, and weight losses were compared using two-way ANOVA. Student's *t*-test was used to determine significant differences in viral loads, and Tukey-Kramer post hoc test was used to discern differences among the groups. $P < 0.05$ was considered statistically significant.

3. Results

### 3.1. AR-12 inhibited the replication of ZIKV strains belonging to both the Asian/American and African lineages

Both the Asian/American and African lineages of ZIKV are considered to be pathogenic and medically important (Musso and Gubler, 2016; Simonin et al., 2016; Zhu et al., 2016). We therefore evaluated the antiviral activity of AR-12 against ZIKV strains belonging to both lineages. In the viral load reduction assay, AR-12 inhibited the replication of all 3 ZIKV strains used in the study, including ZIKV-PR (Asian/American), ZIKV-GD (Asian/American), and ZIKV-U (African), in Huh-7 cells in a dose-dependent manner (Fig. 1). The reduction in viral RNA load of all 3 ZIKV strains was ∼1.0–1.5 logs in culture supernatant and cell lysate of AR-12-treated samples. These findings demonstrated that AR-12 could inhibit both the Asian/American and African lineages of ZIKV.

3.2. AR-12 effectively inhibited multi-cycle replication of ZIKV in vitro

To further characterize the inhibition of ZIKV by AR-12, we prolonged the incubation of Huh-7 cells infected with ZIKV-PR and either AR-12 or DMSO for up to 72 h to study their differential viral kinetics. As shown in Fig. 2, the ZIKV-PR RNA loads in both the culture supernatant and cell lysate of the AR-12-treated samples were consistently ∼1.0–1.5 logs lower than those of the DMSO-treated controls at multiple time points (24, 48, and 72 hpi). The CC_{50}, IC_{50}, and selectivity index of AR-12 in Huh-7 cells were 7.01 μM, 0.82–0.88 μM (culture supernatant and cell lysate), and 7.97–8.55, respectively.

3.3. AR-12 provided cell protection effects against ZIKV infection

In addition to inhibition of viral replication, it was important to determine if cell protection effects against ZIKV infection were present in AR-12-treated cells. In the cell viability assay, a dose-dependent increase in the percentage of viable cells was observed in AR-12-treated Huh-7 cells (Fig. 3). The mean cell viability increased from 55.6% in untreated Huh-7 cells to approximately 100% in cells treated with 3 μM AR-12, suggesting that AR-12 provided cell protection effects against ZIKV infection.
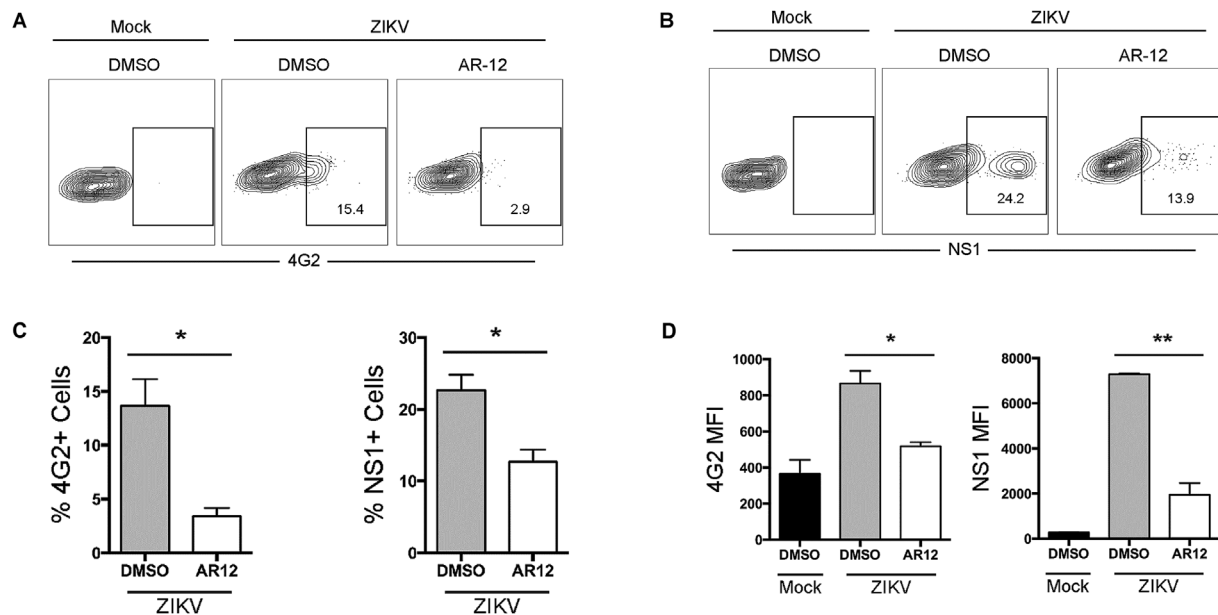
Fig. 6. AR-12 inhibits the antigen expression of ZIKV-PR in U251 cells. U251 cells were infected with ZIKV-PR at 0.5 MOI or were mock-infected for 1 h at 37 °C. The infected cells were subsequently treated with 3 μM AR-12 or DMSO for 24 h. At 24 hpi, the cells were harvested and immunolabeled for flow cytometry analysis. The expression level of ZIKV envelope protein (A) and non-structural 1 protein (B) were labeled with mouse anti-4G2 and mouse anti-NS1, respectively. The percentage of 4G2 or NS1 positive cells (C) and the mean fluorescent intensity (D) were quantified. All experiments were performed in triplicates in three independent experiments for confirmation. * denotes $P < 0.05$ and ** denotes $P < 0.01$ (compared with the DMSO control group by Student's *t*-test). Data are presented as mean values ± standard deviations (error bars). Abbreviations: DMSO, dimethyl sulfoxide; hpi, hours post-inoculation; MFI, mean fluorescence intensity; NS1, non-structural protein 1; ZIKV, Zika virus.

3.4. AR-12 inhibited ZIKV replication in multiple cell types

The major clinical manifestations of ZIKV infection, such as congenital microcephaly and meningoencephalitis, mainly involve neuronal cells. To confirm the observation in the viral load reduction assay using Huh-7 cells, we further evaluated the antiviral activity of AR-12 against the epidemic ZIKV-PR strain in two neuronal (glioblastoma) cell lines, namely, U251 and SF268. As shown in Fig. 4, the ZIKV-PR RNA load was significantly reduced by AR-12 in both U251 ($P < 0.01$) and SF268 cells ($P < 0.001$). The CC_{50}, IC_{50}, and selectivity index of AR-12 in U251 cells were 6.99 μM, 0.84 μM, and 8.32, respectively, and those in SF268 cells were 11.00 μM, 1.18 μM, and 9.32, respectively. The antiviral activity of AR-12 against ZIKV was confirmed even at high MOI by both qRT-PCR and plaque assays (Fig. 5). We next further evaluated the impact of AR-12 on the antigen expression of ZIKV-PR in neuronal cells with flow cytometry (Fig. 6). Remarkably, our result demonstrated that AR-12 significantly inhibited the expression of both the envelope protein (Fig. 6A) and non-structural protein 1 (Fig. 6B) of ZIKV-PR in the infected cells. The inhibition was evidenced by the reduction in the percentage of positive cells (Fig. 6C) as well as the reduction in the mean fluorescent intensity (Fig. 6D).

3.5. AR-12 treatment improved clinical and virological outcome of ZIKV-infected A129 mice

To assess the *in vivo* anti-ZIKV activity of AR-12, we infected type I interferon-receptor-deficient A129 mice with ZIKV-PR and treated them with either AR-12 or sham treatment. The ZIKV-infected mice treated with AR-12 early after infection (1 hpi) had less mean body weight loss ($< 10\%$) (Fig. 7A) and significantly higher survival rate (83.3% vs 0%, $P < 0.001$) (Fig. 7B) than the untreated ZIKV-infected controls. Moreover, the mean ZIKV RNA loads in the blood and necropsied tissues of these AR-12-treated mice at necropsy were generally 0.8–1.5 logs lower than those of the untreated mice (Fig. 7C). We also evaluated regimens of delayed administration of AR-12 either intraperitoneally or by oral gavage to ZIKV-infected mice at 48 hpi to more closely mimic

clinical situations in which viremic patients do not receive treatment immediately after infection. The improved clinical and virological parameters were more obvious in the mice treated with the oral regimen, which consisted of a much higher dose (200 mg/kg) of AR-12 than the intraperitoneal regimen (25 mg/kg) (Fig. 7). These findings illustrated that AR-12 not only inhibited ZIKV *in vitro*, but also *in vivo*, especially if given early or at a high dose.

3.6. AR-12 inhibited ZIKV replication via down-regulation of Akt

Downregulation of 78 kDa glucose-regulated protein (GRP-78) and/or Akt has been previously proposed to be the anti-DENV mechanism of AR-12 (Chen et al., 2017). Surprisingly, in contrast to this previous report, we did not find AR-12 to be downregulating GRP-78 (Fig. 8A). Instead, we found that AR-12 substantially downregulated the phosphorylation of the Akt protein (Fig. 8B). In this regard, our data suggested that AR-12 potentially inhibited ZIKV replication by negatively regulating the Akt signaling pathway. To further investigate if the Akt signaling pathway modulated ZIKV replication, we treated ZIKV-infected Huh-7 cells with an Akt inhibitor, Akt inhibitor VIII, which has been previously shown to inhibit Akt activation (Lindsley et al., 2005). Interestingly, our result demonstrated that ZIKV replication was significantly ($P < 0.05$) inhibited in the presence of Akt inhibitor VIII (Fig. 8C). The involvement of the Akt signaling pathway in ZIKV replication was further validated with siRNA knockdown (Fig. 8D). Akt knockdown resulted in a significant ($P < 0.01$) decrease in ZIKV replication, which was in agreement with the result of the Akt inhibitor VIII experiment (Fig. 8E). Taken together, these findings suggested that AR-12 inhibits ZIKV replication through downregulation of the Akt signaling pathway.

4. Discussion

Drug compounds that target common host pathways involved in the replication cycles of different viruses have the potential advantage of being broad-spectrum antivirals (Zumla et al., 2016). This is especially
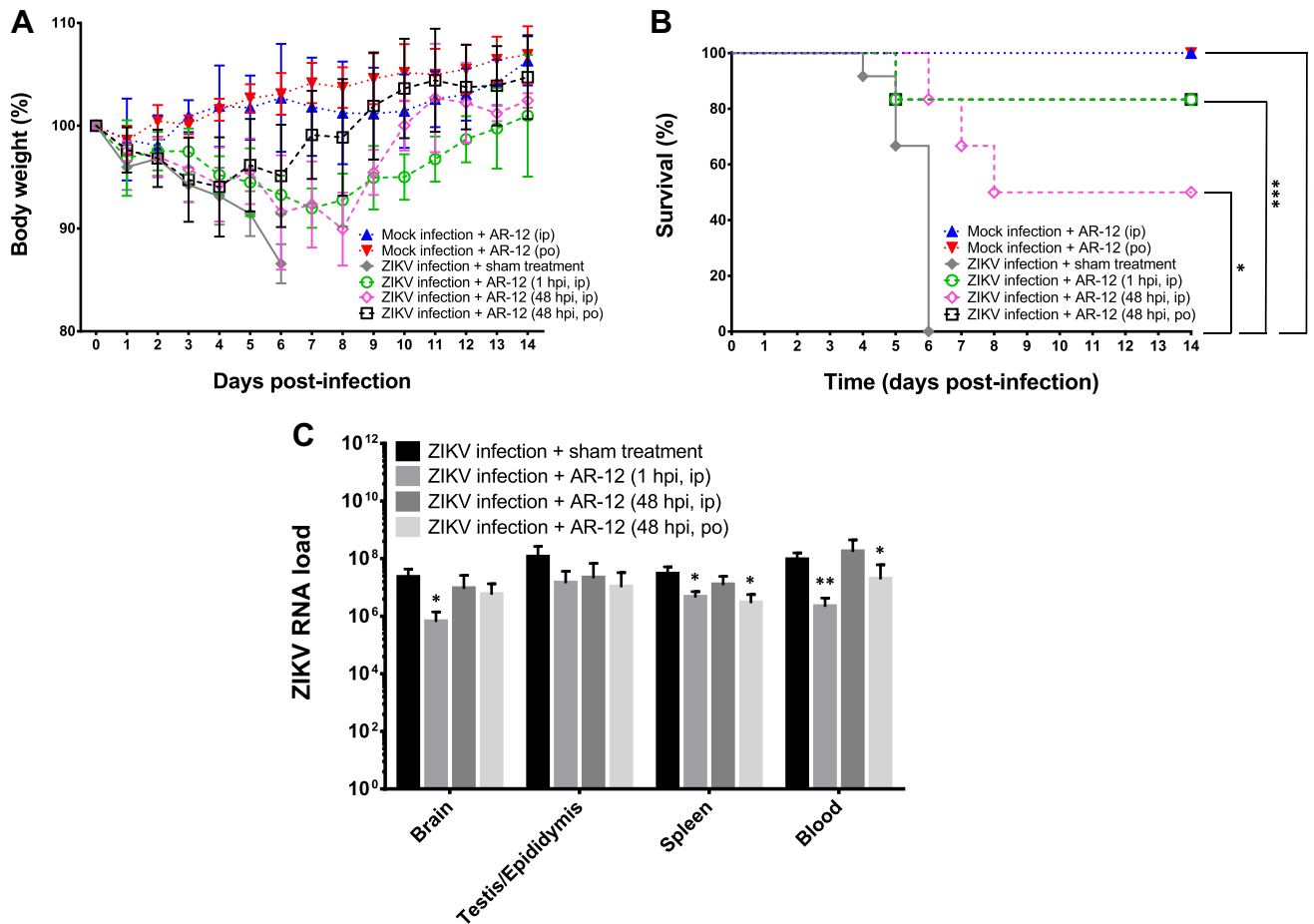
Fig. 7. AR-12 treatment improves clinical and virological outcome of ZIKV-infected A129 mice. (A) Body weight trend, (B) survival rate, and (C) blood and tissue ZIKV RNA loads in the AR-12-treated ZIKV-infected and untreated A129 mice. The mice were treated with 1 dose of 25 mg/kg AR-12 intraperitoneally at 1 hpi, 25 mg/kg AR-12 intraperitoneally at 48 hpi, 200 mg/kg orally AR-12 at 48 hpi, or sham treatment (PBS) (Table S1). Six (12 for sham treatment controls) mice in each group were euthanized when there was ≥20% weight loss or ≥10% weight loss with ≥1 clinical sign or at 6 dpi for blood and organ tissue collection. ZIKV RNA loads in the blood (copies/ml) and tissues (copies/10^6 β-actin) (C) of the mice were determined by qRT-PCR. The body weight and the survival rate of the other mice were monitored from 0 to 14 dpi or until death/euthanasia. The results were combined from four independent experiments. The body weight trends represented those of the survived mice. Statistical significance in (C) represented the difference between the individual treatment groups with the sham treatment control group. * denotes P-values of < 0.05, ** denotes P-values of < 0.01, and *** denotes P-values of < 0.001. Data are presented as mean values ± standard deviations (error bars). Abbreviations: ip, intraperitoneal; PBS, phosphate-buffered saline; po, per os; ZIKV, Zika virus.

important for arboviruses such as ZIKV, DENV, and Chikungunya virus, which co-circulate in the same geographical regions and/or have similar clinical features. We and others have previously identified a number of clinically approved drugs, such as novobiocin, lopinavir-ritonavir, ribavirin, and sofosbuvir, to have anti-ZIKV activity *in vitro* and/or *in vivo* (Bullard-Feibelman et al., 2016; Kamiyama et al., 2017; Yuan et al., 2017). These repurposed drugs directly target the virus by inhibition of key viral enzymes, such as the viral protease and polymerase, and may not have antiviral activity against other co-circulating arboviruses with structurally different viral enzymes.

Host-targeting treatment options for ZIKV remain scarce. We have previously shown the *in vitro* and *in vivo* anti-ZIKV activity of recombinant interferons, but their side effect profiles may limit their clinical use, especially in pregnant women (Chan et al., 2017a; Chan et al., 2016d). A recent study reported the *in vitro* anti-ZIKV activity of a protein kinase A inhibitor (PKI 14–22) in endothelial cells and astrocytes. Another recent study reported that the activation of adenosine monophosphate-activated protein kinase by a small molecule activator (PF-06409577) inhibited ZIKV replication through modulation of host cell lipid metabolism (Jiménez de Oya et al., 2018). These findings supported our hypothesis that drugs which target host signaling pathways may be useful for treating ZIKV infection (Cheng et al., 2018).

During the preparation of this work, AR-12 and a few other kinase inhibitors were recently identified to exhibit *in vitro* anti-ZIKV activity in human osteosarcoma (U2OS) cells in a drug screening programme (Rausch et al., 2017). However, no further validation of this preliminary finding in other clinically relevant cell lines or suitable animal model was reported, and the anti-ZIKV mechanism of AR-12 was not investigated. In this study, we demonstrated the anti-ZIKV activity of AR-12 *in vitro* and *in vivo*, and provided novel insights into the drug's anti-ZIKV mechanism.

We first showed that AR-12 inhibited the replication of ZIKV belonging to both the American/Asian and African lineages. This was important as both lineages of ZIKV are considered to be pathogenic to human. Moreover, treatment with AR-12 provided cell protection effects against ZIKV-induced damage. The anti-ZIKV activity of AR-12 was then validated in multiple cell types, including neuronal cells which are clinically relevant for the neurotropic ZIKV. Importantly, type I interferon receptor-deficient A129 mice treated with AR-12 (either early or delayed regimen) had significantly higher survival rates and lower viral loads than untreated mice, suggesting that the anti-ZIKV effect of AR-12 was not only present *in vitro,* but also in a lethal animal model. We further demonstrated that AR-12 inhibited the phosphorylation of Akt, which is a downstream component of the PI3K/
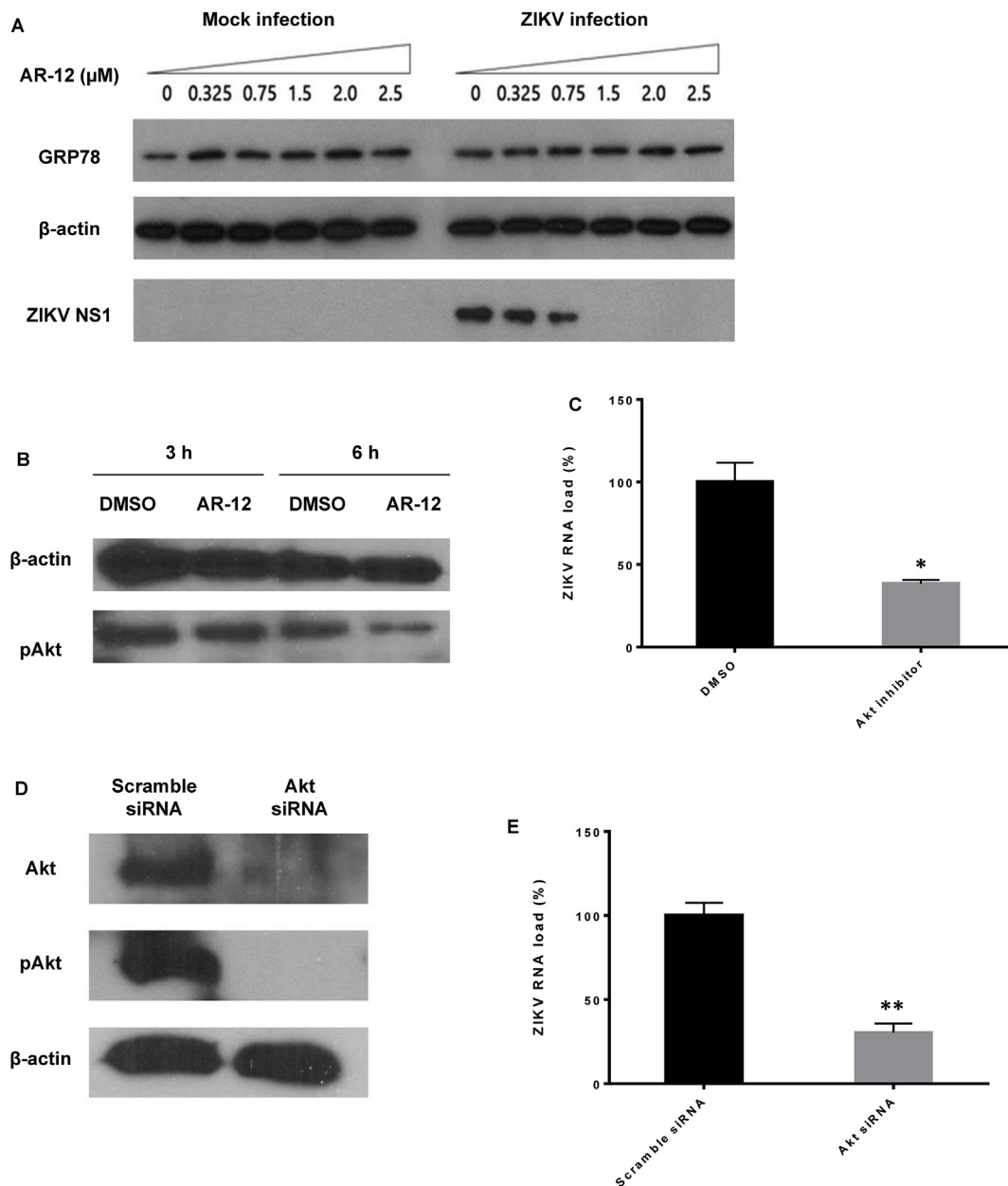
Fig. 8. AR-12 inhibits ZIKV replication via down-regulation of Akt. AR-12 did not downregulate the expression of GRP-78 (A), but reduced Akt phosphorylation (B). Addition of Akt Inhibitor VIII (C) significantly reduced ZIKV RNA load. Similarly, Akt siRNA used in this study downregulated the expression levels of Akt and pAkt (D) and significantly reduced ZIKV RNA load (E). All experiments were performed in triplicates in three independent experiments for confirmation. * denotes $P < 0.05$ and ** denotes $P < 0.01$ (compared with the DMSO or scramble siRNA control groups by Student's *t*-test). Data in Fig. 8C and E are presented as mean values ± standard deviations (error bars). Abbreviations: Akt, protein kinase B; DMSO, dimethyl sulfoxide; GRP-78, 78 kDA glucose-regulated protein; NS1, non-structural protein 1; pAkt, phosphorylated protein kinase B; ZIKV, Zika virus.

Akt signaling pathway that promotes flavivirus replication by counteracting virus-induced cellular apoptosis.

The ZIKV RNA load reduction (~1.0–1.5 logs) observed in our cell culture systems and animal model with AR-12 treatment is comparable with previous findings on AR-12's antiviral effects against other RNA viruses. For example, the CC_{50}, IC_{50}, and selectivity index values of AR-12 against other hemorrhagic fever viruses were comparable with our findings for ZIKV (Mohr et al., 2015). For flaviviruses, there was about 1 log reduction of DENV RNA load with 2–4 μM AR-12 and the IC_{50} values of AR-12 against DENV serotypes 1–4 were between 0.60 μM and 0.80 μM in Vero cells (Hassandarvish et al., 2017). The CC_{50} of AR-12 was higher in Vero cells (65.90 μM) than in our Huh-7 and neuronal cells, suggesting that the selectivity index of AR-12 against flaviviruses may be even higher in other cell types (up to > 100) (Hassandarvish

et al., 2017). In DENV-infected suckling mice treated with AR-12 intracranially and intraperitoneally, there was about 0.5–0.7 log reduction in infectious virus particles (plaque forming units) in their brain tissues (Chen et al., 2017). In comparison, virus-targeting drugs often achieve a higher degree of viral load reduction (> 2 logs) *in vitro* and *in vivo*. For example, the ZIKV NS2B-NS3 protease inhibitor novobiocin reduces ZIKV RNA load by ≥ 2 logs both *in vitro* (Vero and Huh-7 cells) and in the blood and tissues of ZIKV-infected mice (Yuan et al., 2017). Our recently described antiviral peptide (Z2 peptide) targeting the stem region of the ZIKV envelope protein to inhibit virus entry into host cells significantly reduced viral RNA load in ZIKV-infected interferon receptor-deficient mice and inhibited vertical transmission of ZIKV in pregnant C57BL/6 mice (Yu et al., 2017). These findings are not un-expected as our mice only received one dose of AR-12 treatment post-

infection and because AR-12's antiviral mechanism via downregulation of the PI3K/Akt signaling pathway is not as direct as those of virus-targeting drugs.

AR-12 has the advantages of being broad-spectrum and orally available, and may be clinically useful as an empirical therapy before laboratory diagnosis is established in patients living in or returning from endemic areas of arboviral and hemorrhagic fever viral diseases who develop an acute febrile illness. The effect of AR-12 as part of combination treatment regimens consisting of both virus-targeting and host-targeting drugs should be evaluated in future studies, as this treatment strategy may be associated with improved clinical outcomes for ZIKV and other RNA viral infections (Hung et al., 2017; Pires de Mello et al., 2017; Zumla et al., 2016). Further optimization of the delivery of AR-12, such as encapsulation of the drug into biodegradable polymeric nanoparticles to reduce cytotoxicity and increase drug concentration per cell may facilitate its use in these clinical settings (Collier et al., 2016; Hoang et al., 2016).

Author contributions

J.F.-W.C., Z.Z., H.C., and K.-Y.Y. designed the study. Z.Z., H.C., S.Y., K.K.-H.C., C.C.-S.C., V.K.-M.P., C.C.-Y.Y., X.Z., J.O.-L.T., Z.Z., K.-M.T., and H.S. performed the experiments. J.F.-W.C., Z.Z., H.C., G.L., and K.-Y.Y. performed data analysis and interpretation. J.F.-W.C., Z.Z., H.C., and K.-Y.Y. wrote the manuscript.

Conflicts of interest

J.F.-W.C. has received travel grants from Pfizer Corporation Hong Kong and Astellas Pharma Hong Kong Corporation Limited, and was an invited speaker for Gilead Sciences Hong Kong Limited and Luminex Corporation. The other authors declared no conflict of interests. The funding sources had no role in study design, data collection, analysis or interpretation or writing of the report. The corresponding authors had full access to all the data in the study and had final responsibility for the decision to submit for publication.

Appendix A. Supplementary data

Supplementary data to this article can be found online at doi:https://doi.org/10.1016/j.antiviral.2018.10.007.

References

Booth, L., Shuch, B., Albers, T., Roberts, J.L., Tavallai, M., Proniuk, S., Zukiwski, A., Wang, D., Chen, C.S., Bottaro, D., et al., 2016. Multi-kinase inhibitors can associate with heat shock proteins through their NH2-termini by which they suppress chaperone function. Oncotarget 7, 12975–12996.

Bullard-Feibelman, K.M., Govero, J., Zhu, Z., Salazar, V., Veselinovic, M., Diamond, M.S., Geiss, B.J., 2016. The FDA-approved drug sofosbuvir inhibits Zika virus infection. Antivir. Res. 137, 134–140.

Chan, C.M., Chu, H., Wang, Y., Wong, B.H., Zhao, X., Zhou, J., Yang, D., Leung, S.P., Chan, J.F., Yeung, M.L., et al., 2016a. Carcinoembryonic antigen-related cell adhesion molecule 5 is an important surface attachment factor that facilitates entry of Middle East respiratory syndrome coronavirus. J. Virol. 90, 9114–9127.

Chan, J.F., Chan, K.H., Kao, R.Y., To, K.K., Zheng, B.J., Li, C.P., Li, P.T., Dai, J., Mok, F.K., Chen, H., et al., 2013a. Broad-spectrum antivirals for the emerging Middle East respiratory syndrome coronavirus. J. Infect. 67, 606–616.

Chan, J.F., Chik, K.K., Yuan, S., Yip, C.C., Zhu, Z., Tee, K.M., Tsang, J.O., Chan, C.C., Poon, V.K., Lu, G., et al., 2017a. Novel antiviral activity and mechanism of bromocriptine as a Zika virus NS2B-NS3 protease inhibitor. Antivir. Res. 141, 29–37.

Chan, J.F., Choi, G.K., Yip, C.C., Cheng, V.C., Yuen, K.Y., 2016b. Zika fever and congenital Zika syndrome: an unexpected emerging arboviral disease. J. Infect. 72, 507–524.

Chan, J.F., Lau, S.K., To, K.K., Cheng, V.C., Woo, P.C., Yuen, K.Y., 2015. Middle East respiratory syndrome coronavirus: another zoonotic betacoronavirus causing SARS-like disease. Clin. Microbiol. Rev. 28, 465–522.

Chan, J.F., To, K.K., Tse, H., Jin, D.Y., Yuen, K.Y., 2013b. Interspecies transmission and emergence of novel viruses: lessons from bats and birds. Trends Microbiol. 21, 544–555.

Chan, J.F., Yip, C.C., Tee, K.M., Zhu, Z., Tsang, J.O., Chik, K.K., Tsang, T.G., Chan, C.C., Poon, V.K., Sridhar, S., et al., 2017b. Improved detection of Zika virus RNA in human and animal specimens by a novel, highly sensitive and specific real-time RT-PCR assay targeting the 5'-untranslated region of Zika virus. Trop. Med. Int. Health 22, 594–603.

Chan, J.F., Yip, C.C., Tsang, J.O., Tee, K.M., Cai, J.P., Chik, K.K., Zhu, Z., Chan, C.C., Choi, G.K., Sridhar, S., et al., 2016c. Differential cell line susceptibility to the emerging Zika virus: implications for disease pathogenesis, non-vector-borne human transmission and animal reservoirs. Emerg. Microb. Infect. 5, e93.

Chan, J.F., Zhang, A.J., Chan, C.C., Yip, C.C., Mak, W.W., Zhu, H., Poon, V.K., Tee, K.M., Zhu, Z., Cai, J.P., et al., 2016d. Zika virus infection in dexamethasone-immunosuppressed mice demonstrating disseminated infection with multi-organ involvement including orchitis effectively treated by recombinant type I interferons. EBioMedicine 14, 112–122.

Chen, H.H., Chen, C.C., Lin, Y.S., Chang, P.C., Lu, Z.Y., Lin, C.F., Chen, C.L., Chang, C.P., 2017. AR-12 suppresses dengue virus replication by down-regulation of PI3K/AKT and GRP78. Antivir. Res. 142, 158–168.

Cheng, F., Ramos da Silva, S., Huang, I.C., Jung, J.U., Gao, S.J., 2018. Suppression of Zika virus infection and replication in endothelial cells and astrocytes by PKA inhibitor PKI 14-22. J. Virol. 92.

Chiu, H.C., Kulp, S.K., Soni, S., Wang, D., Gunn, J.S., Schlesinger, L.S., Chen, C.S., 2009a. Eradication of intracellular Salmonella enterica serovar Typhimurium with a small-molecule, host cell-directed agent. Antimicrob. Agents Chemother. 53, 5236–5244.

Chiu, H.C., Soni, S., Kulp, S.K., Curry, H., Wang, D., Gunn, J.S., Schlesinger, L.S., Chen, C.S., 2009b. Eradication of intracellular Francisella tularensis in THP-1 human macrophages with a novel autophagy inducing agent. J. Biomed. Sci. 16, 110.

Chu, J.J., Yang, P.L., 2007. c-Src protein kinase inhibitors block assembly and maturation of dengue virus. Proc. Natl. Acad. Sci. U. S. A 104, 3520–3525.

Chu, H., Zhou, J., Wong, B.H., Li, C., Chan, J.F., Cheng, Z.S., Yang, D., Wang, D., Lee, A.C., Li, C., et al., 2016. Middle East respiratory syndrome coronavirus efficiently infects human primary T lymphocytes and activates the extrinsic and intrinsic apoptosis pathways. J. Infect. Dis. 213, 904–914.

Chu, H., Zhou, J., Wong, B.H., Li, C., Cheng, Z.S., Lin, X., Poon, V.K., Sun, T., Lau, C.C., Chan, J.F., et al., 2014. Productive replication of Middle East respiratory syndrome coronavirus in monocyte-derived dendritic cells modulates innate immune response. Virology 454–455, 197–205.

Collier, M.A., Peine, K.J., Gautam, S., Oghumu, S., Varikuti, S., Borteh, H., Papenfuss, T.L., Sataoskar, A.R., Bachelder, E.M., Ainslie, K.M., 2016. Host-mediated Leishmania donovani treatment using AR-12 encapsulated in acetalated dextran microparticles. Int. J. Pharm. 499, 186–194.

Dowall, S.D., Graham, V.A., Rayner, E., Atkinson, B., Hall, G., Watson, R.J., Bosworth, A., Bonney, L.C., Kitchen, S., Hewson, R., 2016. A Susceptible Mouse Model for Zika Virus Infection. PLoS Neglected Trop. Dis. 10, e0004658.

Duffy, M.R., Chen, T.H., Hancock, W.T., Powers, A.M., Kool, J.L., Lanciotti, R.S., Pretrick, M., Marfel, M., Holzbauer, S., Dubray, C., et al., 2009. Zika virus outbreak on Yap island, Federated States of Micronesia. N. Engl. J. Med. 360, 2536–2543.

Guo, Q., Chan, J.F., Poon, V.K., Wu, S., Chan, C.C., Hou, L., Yip, C.C., Ren, C., Cai, J.P., Zhao, M., et al., 2018. Immunization with a novel human type 5 adenovirus-vectored vaccine expressing the premembrane and envelope proteins of Zika virus provides consistent and sterilizing protection in multiple immunocompetent and immunocompromised animal models. J. Infect. Dis. 218, 365–377.

Hassandarvish, P., Oo, A., Jokar, A., Zukiwski, A., Proniuk, S., Abu Bakar, S., Zandi, K., 2017. Exploring the in vitro potential of celecoxib derivative AR-12 as an effective antiviral compound against four dengue virus serotypes. J. Antimicrob. Chemother. 72 (2017), 2438–2442.

Hoang, K.V., Curry, H., Collier, M.A., Borteh, H., Bachelder, E.M., Schlesinger, L.S., Gunn, J.S., Ainslie, K.M., 2016. Needle-free delivery of acetalated dextran-encapsulated AR-12 protects mice from Francisella tularensis lethal challenge. Antimicrob. Agents

Chemother. 60, 2052–2062.

Hung, I.F.N., To, K.K.W., Chan, J.F.W., Cheng, V.C.C., Liu, K.S.H., Tam, A., Chan, T.C., Zhang, A.J., Li, P., Wong, T.L., et al., 2017. Efficacy of clarithromycin-naproxen-oseltamivir combination in the treatment of patients hospitalized for influenza A(H3N2) infection: an open-label randomized, controlled, phase IIb/III trial. Chest 151, 1069–1080.

Jiménez de Oya, N., Blázquez, A.B., Casas, J., Saiz, J.C., Martín Acebes, M.A., 2018. Direct activation of adenosine monophosphate-activated protein kinase (AMPK) by PF-06409577 inhibits flavivirus infection through modification of host-cell lipid metabolism. pii: AAC.00360-18. Antimicrob. Agents Chemother. https://doi.org/10.1128/AAC.00360-18. ([Epub ahead of print]).

Kamiyama, N., Soma, R., Hidano, S., Watanabe, K., Umekita, H., Fukuda, C., Noguchi, K., Gendo, Y., Ozaki, T., Sonoda, A., et al., 2017. Ribavirin inhibits Zika virus (ZIKV) replication in vitro and suppresses viremia in ZIKV-infected STAT1-deficient mice. Antivir. Res. 146, 1–11.

Koselny, K., Green, J., DiDone, L., Halterman, J.P., Fothergill, A.W., Wiederhold, N.P., Patterson, T.F., Cushion, M.T., Rappelye, C., Wellington, M., et al., 2016. The celecoxib derivative AR-12 has broad-spectrum antifungal activity in vitro and improves the activity of fluconazole in a murine model of cryptococcosis. Antimicrob. Agents Chemother. 60, 7115–7127.

Lee, C.J., Liao, C.L., Lin, Y.L., 2005. Flavivirus activates phosphatidylinositol 3-kinase signaling to block caspase-dependent apoptotic cell death at the early stage of virus infection. J. Virol. 79, 8388–8399.

Lee, T.X., Packer, M.D., Huang, J., Akhmametyeva, E.M., Kulp, S.K., Chen, C.S., Giovannini, M., Jacob, A., Welling, D.B., Chang, L.S., 2009. Growth inhibitory and anti-tumour activities of OSU-03012, a novel PDK-1 inhibitor, on vestibular schwannoma and malignant schwannoma cells. Eur. J. Canc. 45, 1709–1720.

Lindsley, C.W., Zhao, Z., Leister, W.H., Robinson, R.G., Barnett, S.F., Defeo-Jones, D., Jones, R.E., Hartman, G.D., Huff, J.R., Huber, H.E., et al., 2005. Allosteric Akt (PKB) inhibitors: discovery and SAR of isozyme selective inhibitors. Bioorg. Med. Chem. Lett 15, 761–764.

Linero, F.N., Scolaro, L.A., 2009. Participation of the phosphatidylinositol 3-kinase/Akt pathway in Junin virus replication in vitro. Virus Res. 145, 166–170.

MacNeil, A., Rollin, P.E., 2012. Ebola and Marburg hemorrhagic fevers: neglected tropical diseases? PLoS Neglected Trop. Dis. 6, e1546.

Marsh, G.A., Wang, L.F., 2012. Hendra and Nipah viruses: why are they so deadly? Curr. Opin. Virol. 2, 242–247.

Mohr, E.L., McMullan, L.K., Lo, M.K., Spengler, J.R., Bergeron, É., Albariño, C.G., Shrivastava-Ranjan, P., Chiang, C.F., Nichol, S.T., Spiropoulou, C.F., et al., 2015. Inhibitors of cellular kinases with broad-spectrum antiviral activity for hemorrhagic fever viruses. Antivir. Res. 120, 40–47.

Musso, D., Gubler, D.J., 2016. Zika virus. Clin. Microbiol. Rev. 29, 487–524.

Pires de Mello, C.P., Tao, X., Kim, T.H., Bulitta, J.B., Rodriquez, J.L., Pomeroy, J.J., Brown, A.N., 2017. Zika virus replication is substantially inhibited by novel favipiravir and interferon alpha combination regimens. Antimicrob. Agents Chemother. 2017, 62.

Rausch, K., Hackett, B.A., Weinbren, N.L., Reeder, S.M., Sadovsky, Y., Hunter, C.A., Schultz, D.C., Coyne, C.B., Cherry, S., 2017. Screening bioactives reveals nanchangmycin as a broad spectrum antiviral active against Zika virus. Cell Rep. 18, 804–815.

Saeed, M.F., Kolokoltsov, A.A., Freiberg, A.N., Holbrook, M.R., Davey, R.A., 2008. Phosphoinositide-3 kinase-Akt pathway controls cellular entry of Ebola virus. PLoS Pathog. 4, e1000141.

Simonin, Y., Loustalot, F., Desmetz, C., Foulongne, V., Constant, O., Fournier-Wirth, C., Leon, F., Molès, J.P., Goubaud, A., Lemaître, J.M., et al., 2016. Zika virus strains potentially display different infectious profiles in human neural cells. EBioMedicine 12, 161–169.

To, K.K., Chan, J.F., Chen, H., Li, L., Yuen, K.Y., 2013. The emergence of influenza A H7N9 in human beings 16 years after influenza A H5N1: a tale of two cities. Lancet Infect. Dis. 13, 809–821.

To, K.K., Chan, J.F., Tsang, A.K., Cheng, V.C., Yuen, K.Y., 2015. Ebola virus disease: a highly fatal infectious disease reemerging in West Africa. Microb. Infect. 17, 84–97.

Tsai, T.T., Chuang, Y.J., Lin, Y.S., Chang, C.P., Wan, S.W., Lin, S.H., Chen, C.L., Lin, C.F., 2014. Antibody-dependent enhancement infection facilitates dengue virus-regulated signaling of IL-10 production in monocytes. PLoS Neglected Trop. Dis. 8, e3320.

Urata, S., Ngo, N., de la Torre, J.C., 2012. The PI3K/Akt pathway contributes to arenavirus budding. J. Virol. 86, 4578–4585.

Yu, Y., Deng, Y.Q., Zou, P., Wang, Q., Dai, Y., Yu, F., Du, L., Zhang, N.N., Tian, M., Hao, J.N., et al., 2017. A peptide-based viral inactivator inhibits Zika virus infection in pregnant mice and fetuses. Nat. Commun. 8, 15672.

Yuan, S., Chan, J.F., den-Haan, H., Chik, K.K., Zhang, A.J., Chan, C.C., Poon, V.K., Yip, C.C., Mak, W.W., Zhu, Z., et al., 2017. Structure-based discovery of clinically approved drugs as Zika virus NS2B-NS3 protease inhibitors that potently inhibit Zika virus infection in vitro and in vivo. Antivir. Res. 145, 33–43.

Zhu, Z., Chan, J.F., Tee, K.M., Choi, G.K., Lau, S.K., Woo, P.C., Tse, H., Yuen, K.Y., 2016. Comparative genomic analysis of pre-epidemic and epidemic Zika virus strains for virological factors potentially associated with the rapidly expanding epidemic. Emerg. Microb. Infect. 5, e22.

Zumla, A., Chan, J.F., Azhar, E.I., Hui, D.S., Yuen, K.Y., 2016. Coronaviruses - drug discovery and therapeutic options. Nat. Rev. Drug Discov. 15, 327–347.